BIOCHEMISTRY
including biophysical chemistry & molecular biology

Article

pubs.acs.org/biochemistry

Comparison of Membrane Insertion Pathways of the Apoptotic Regulator Bcl-xL and the Diphtheria Toxin Translocation Domain

Mauricio Vargas-Uribe, Mykola V. Rodnin, and Alexey S. Ladokhin*

Department of Biochemistry and Molecular Biology, University of Kansas Medical Center, Kansas City, Kansas 66160, United States

Supporting Information

ABSTRACT: The diphtheria toxin translocation domain (T-domain) and the apoptotic repressor Bcl-xL are membrane proteins that adopt their final topology by switching folds from a water-soluble to a membrane-inserted state. While the exact molecular mechanisms of this transition are not clearly understood in either case, the similarity in the structures of soluble states of the T-domain and Bcl-xL led to the suggestion that their membrane insertion pathways will be similar, as well. Previously, we have applied an array of spectroscopic methods to characterize the pH-triggered refolding and membrane insertion of the diphtheria toxin T-domain. Here, we use the same set of methods to describe the membrane insertion pathway of Bcl-xL, which allows us to make a direct comparison between both systems with respect to the thermodynamic stability in solution, pH-dependent membrane association, and transmembrane insertion. Thermal denaturation measured by circular dichroism indicates that, unlike the T-domain, Bcl-xL does not undergo a pH-dependent destabilization of the structure. Förster resonance energy transfer measurements demonstrate that Bcl-xL undergoes reversible membrane association modulated by the presence of anionic lipids, suggesting that formation of the membrane-competent form occurs close to the membrane interface. Membrane insertion of the main hydrophobic helical hairpin of Bcl-xL, α5−α6, was studied by site-selective attachment of environment-sensitive dye NBD. In contrast to the insertion of the corresponding TH8−TH9 hairpin into the T-domain, insertion of α5−α6 was found not to depend strongly on the presence of anionic lipids. Taken together, our results indicate that while Bcl-xL and the T-domain share structural similarities, their modes of conformational switching and membrane insertion pathways are distinctly different.

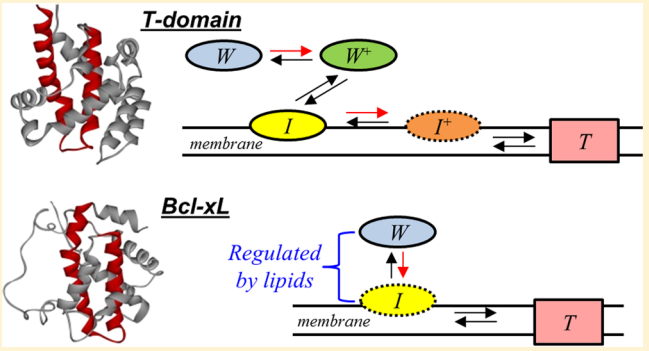

Several classes of membrane proteins adopt their transmembrane topology posttranslationally, where they are synthesized as water-soluble structures that later insert into the bilayer in response to a given cellular signal. Examples include some bacterial toxins[1−3] and colicins,[4] which are secreted to the extracellular space, and certain annexins[5] and members of the Bcl-2 family of proteins,[6] which are synthesized as cytosolic proteins. The unique characteristic of these proteins is their ability to move from the polar environment of the aqueous medium to the nonpolar milieu of the lipid bilayer, a process that clearly involves a massive refolding of the structure. The exact molecular pathways of this refolding−insertion process are not well understood, and it is not clear if different proteins follow the same pathway or share common features. In this study, we compare the membrane insertion pathways of the diphtheria toxin T-domain and the apoptotic repressor Bcl-xL, two membrane proteins that share structural similarities in their water-soluble state (Figure 1).

The translocation domain (T-domain) plays a crucial role in the action of the diphtheria toxin.[1,2] The toxin, which is composed of three domains, initiates its entry into the target cell by the attachment of the receptor-binding (R) domain to its receptor in the membrane (see the scheme in Figure 2). Upon endosomal internalization and acidification, the T-domain undergoes a series of pH-triggered conformational changes that result in its membrane insertion and the translocation of the catalytic domain (C-domain), which holds the toxic activity, across the bilayer. The crystal structure of the T-domain in solution at neutral pH (Figure 1A) shows two central hydrophobic helices, TH8 and TH9 (red helices), surrounded by amphipathic regions (gray helices and loops). There is no high-resolution structure available for the membrane-inserted state, but the current knowledge suggests that TH8 and TH9 insert as a transmembrane hairpin into the bilayer while the rest of the structure may adopt multiple conformations.[8−12] Previously, we have established the hallmarks of the membrane insertion pathway of the T-domain and the residues responsible for pH-dependent conformational switching.[13−17]

Bcl-xL is an anti-apoptotic member of the Bcl-2 family of proteins whose function is inhibiting the mitochondrial outer membrane permeabilization (MOMP) to prevent the cell from going into apoptosis.[6,18] The mechanism by which Bcl-xL

Received: July 12, 2013
Revised: October 15, 2013
Published: October 17, 2013

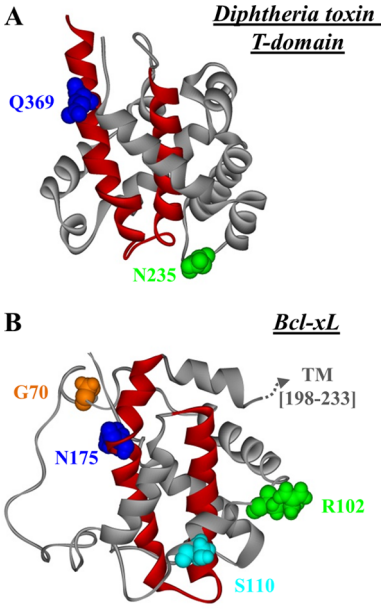

Figure 1. (A) Crystal structure of the diphtheria toxin T-domain [Protein Data Bank (PDB) entry 1MDT] in solution at neutral pH.[7] The central helices TH8 and TH9 are colored red, and residues N235 and Q369, used for cysteine replacement for site-selective labeling in ref 13, are shown as CPK representations. (B) Nuclear magnetic resonance structure of Bcl-xL (PDB entry 1LXL) in solution,[24] highlighting helices α5 and α6 (red) and residues G70, R102, S110, and N175, which were used for cysteine replacement for site-selective labeling in this study. The putative location of the truncated C-terminal transmembrane helix is shown as a dotted arrow.

accomplishes its action is still under debate,[19−21] although it is thought to involve its redistribution between a cytosolic and a membrane-associated form.[22,23] From the structural point of view, Bcl-xL shares significant similarity with the diphtheria toxin T-domain.[24−26] First, the high-resolution structure of Bcl-xL in the water-soluble state[24] shows a highly helical structure (Figure 1B), with two central hydrophobic helices, α5 and α6 (red helices). The remaining helices (gray helices), as in the case of the T-domain, surround the hydrophobic core. Bcl-xL, however, has an additional hydrophobic helix located at the C-terminus, a transmembrane (TM) helix, which is thought to anchor the protein to the membrane prior to insertion.[25] Second, Bcl-xL is able to insert into the bilayer in response to a low pH,[27−30] although it is not clear if this is a prevailing signal that triggers insertion in the cell. Third, it is suggested that Bcl-xL accomplishes its blocking action of Bax (pore-forming member of the Bcl-2 family) by inserting into the bilayer as a monomer.[31] Similarly, the active form of the T-domain also is a monomer.[32,33] Finally, although the high-resolution structure of Bcl-xL in the membrane-inserted state is not available either, it has been suggested that helices α5 and α6 insert as transmembrane regions,[25,34] like TH8 and TH9 of the T-domain, whereas other regions might reside in the membrane interface.

Given the multiple similarities between the toxin and Bcl-xL, it has been proposed that the T-domain serves as model for the understanding of the action of Bcl-xL,[24,26] and by extension of other structurally similar Bcl-2 proteins,[6] on the membrane. Here, we test this hypothesis by applying the same array of spectroscopic methods used in the T-domain studies to characterize the solution refolding and membrane interactions of Bcl-xL and compare them to those of the T-domain.

MATERIALS AND METHODS

Materials. Palmitoyloleoylphosphatidylcholine (POPC), palmitoyloleoylphosphatidylglycerol (POPG), and Rhodamine-PE were purchased from Avanti Polar Lipids (Alabaster, AL). IANBD-ester and AlexaFluor488-maleimide were obtained from Invitrogen (Carlsbad, CA).

Cloning and Mutagenesis. Full-length Bcl-xL (residues 1−233) was amplified via polymerase chain reaction from cDNA obtained from K562 human lymphoma cells and ligated into the pET28b vector using the NdeI and EcoRI cloning sites. The truncated version of Bcl-xL (residues 1−207) was generated by introducing a stop codon at the position corresponding to residue 208. For the purposes of Cys labeling with fluorescent dyes, a Cys-less mutant (C151S) was created and used as a template for site-directed mutagenesis. All the constructs contained an N-terminal six-His tag for purification.

Expression, Purification, and Labeling. The expression and purification of Bcl-xL were based on the previously described procedure for the pET system.[35] Briefly, BL-DE23pLysE *Escherichia coli* cells were transformed with the corresponding pET plasmid and grown to an OD_{600} of ∼0.6, after which expression was induced by the addition of 0.8 M IPTG and the cells were grown for an additional 16 h at 24 °C. The cells were pelleted by centrifugation, lysed by sonication, and clarified by centrifugation for 30 min at 4000 rpm and 4 °C. The proteins were then incubated with Ni-NTA beads, washed with washing buffer [50 mM Tris-HCl, 300 mM NaCl, and 5 mM imidazole (pH 8)], and eluted with 0.5 M imidazole in the same buffer. The eluted proteins were subjected to size-exclusion chromatography on a Sepharose12 1 cm × 30 cm column in 50 mM phosphate buffer (pH 8) and quantified by measuring their absorbance spectra in the range of 200−350 nm (we used a molar extinction coefficient of 41200 M^{-1} cm^{-1} at 280 nm). Labeling with fluorescent dyes was performed using a standard procedure for thiol-reactive derivatives,[13,36] and the unreacted dye was removed by gel filtration chromatography in the same column and buffer.

Preparation of Large Unilamellar Vesicles. Large unilamellar vesicles (LUV) containing POPG/POPC molar mixtures (3:1, 1:3, and 1:9) 0.1 μm in diameter were prepared by extrusion as previously described.[37,38] Rhodamine-labeled LUV were prepared by the addition of 2% Rhodamine-PE to the lipid mixture.

Circular Dichroism (CD) and Thermal Unfolding. CD measurements were performed using an upgraded Jasco-720 spectropolarimeter (Japan Spectroscopic Co., Tokyo, Japan). Normally, 100 scans were recorded between 190 and 260 nm with a 1 nm step at 25 and 95 °C using a 1 mm optical path-length cuvette. The sample contained 4 μM Bcl-xL in 50 mM phosphate buffer (pH 8.0) or a mixture of phosphate and acetic/acetate buffer at pH 6.0, 5.0, or 4.0. Further acidification was achieved by equilibrating the sample in 50 mM glycine-HCl buffer. All spectra were corrected for background. The thermal unfolding was followed at 222 nm at a scan rate of 1 °C/min, unless indicated. The data were fit to a two-state transition as described previously,[15,17] yielding the transition temperature (T_m) and the transition enthalpy ($\Delta H°$).

Fluorescence Measurements and Analysis. Steady-state fluorescence emission was measured using a SPEX Fluorolog FL3-22 steady-state fluorescence spectrometer (Jobin Yvon,

dx.doi.org/10.1021/bi400926k | *Biochemistry* 2013, 52, 7901−7909

Edison, NJ) equipped with double-grating excitation and emission monochromators. The measurements were taken in a 2 mm × 10 mm cuvette oriented perpendicular to the excitation beam and maintained at 25 °C using a Peltier device from Quantum Northwest (Spokane, WA) in 1 nm steps. For Alexa488 measurements, we recorded the emission spectra from 470 to 700 nm with an excitation wavelength of 455 nm and slits of 2 nm for both excitation and emission. For NBD measurements, we collected the emission spectra from 490 to 700 nm and the excitation wavelength was 470 nm, using slits of 5 nm on both monochromators. For each spectrum, we averaged five scans after incubating the samples for 30 min for equilibration.

Fluorescence decays were measured with a time-resolved fluorescence spectrometer (FluoTime 200, PicoQuant, Berlin, Germany), using a standard time-correlated single-photon counting scheme as previously described.[39] Samples were excited at 440 nm by a subnanosecond pulsed diode laser (LDH 440, PicoQuant), with a repetition rate of 10 MHz. Fluorescence emission was detected at 535 nm, selected by a Sciencetech model 9030 monochromator, using a PMA-182 photomultiplier (PicoQuant). The samples normally contained 0.3 μM protein and 0.5 mM lipid. The fluorescence intensity decay was analyzed using FluoFit iterative-fitting software based on the Marquardt algorithm (PicoQuant).

The pH dependencies of the fraction of membrane-bound or membrane-inserted states generated by corresponding spectroscopic experiments were fit to the following equation:[40]

$$F = \frac{1}{1 + 10^{n(\mathrm{pH}-\mathrm{p}K)}} \quad (1)$$

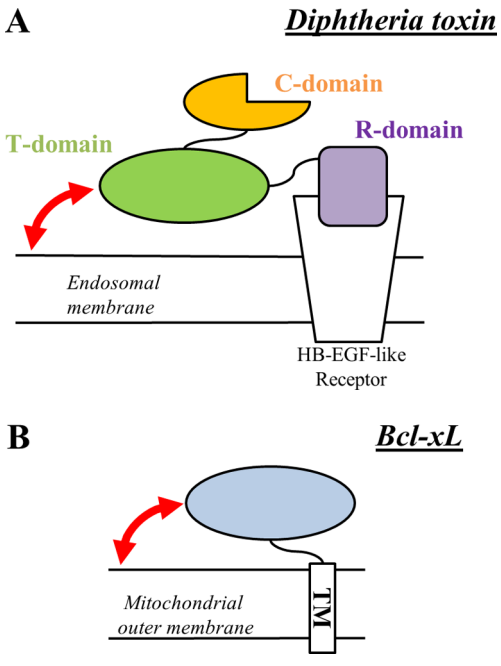

Figure 2. Schematic representation of the mode of attachment of the diphtheria toxin (A) and Bcl-xL (B) to their target membranes. The figure illustrates the equivalent attachment−anchor function of the transmembrane helix and the R-domain for Bcl-xL and the diphtheria toxin, respectively. The membrane insertion of the T-domain and the N-terminal region of Bcl-xL occur regardless of the attachment to the membrane. The processes addressed in this study are shown as curved red arrows (see the text).

where pK is a negative logarithm of the dissociation constant and n is the Hill coefficient.

RESULTS AND DISCUSSION

Choice of Experimental Models for Insertion Studies.

The diphtheria toxin is composed of three domains: the C-domain (residues 1−199), the T-domain (residues 200−378), and the R-domain (residues 379−535). The C-domain inhibits protein synthesis in the target cell and must enter the cytosol to execute its action. The R-domain is responsible for the initial attachment of the toxin to the target cell through a direct interaction with a membrane receptor (Figure 2A). The membrane insertion of the T-domain and translocation of the C-domain across the bilayer, however, do not take place at this point, because the T-domain requires the acidification of the medium, which occurs at a later stage inside the endosome.[1] As a consequence, the T-domain retains the water-soluble structure regardless of the attachment of the entire toxin to the membrane. The isolated T-domain has been shown to be able to translocate its own terminus in model membrane systems (along with the C-domain, if attached[41]) as well as to ensure translocation of various molten globule-like proteins.[42] Hence, the isolated T-domain has been a choice model for numerous biophysical studies of membrane binding and insertion.[8−17,33,43−46]

What would be an appropriate version of Bcl-xL to be compared to the T-domain with regard to membrane insertion? The initial attachment of Bcl-xL to the mitochondrial membrane is ensured by a single TM helical fragment (residues 208−233). The folded N-terminal region (oval in Figure 2B) remains in a water-soluble state[25] and does not enter the membrane prior to the activation, which at least in model systems can be achieved by a change in pH.[27−30] This arrangement is similar to that of the diphtheria toxin, with the TM fragment and the N-terminal domain of Bcl-xL being equivalent to the R-domain and the T-domain of the toxin, respectively. Therefore, most of our results were generated with a Bcl-xL version in which the C-terminal TM helix has been truncated. Thus, the comparison made in this study corresponds to the membrane binding and insertion processes of the N-terminal domain of Bcl-xL (residues 1−207) and the isolated T-domain (residues 200−378), depicted as curved arrows in Figure 2.

The truncation of the TM helix in Bcl-xL offers important additional advantages because it allows the study of the initial association of the protein with the membrane interface. The Förster resonance energy transfer (FRET) assay used in this study for measuring this association was developed, and validated using independent FCS measurements, for the case of the T-domain.[13] The assay uses the donor in the protein and the acceptor attached to a lipid headgroup and requires that the protein and the membrane interface not be within the Förster distance of the donor−acceptor pair prior to the interaction. If the protein is already anchored to the bilayer because of the TM helix, then the donor and acceptor would be within the Förster distance, and no spectral changes can be observed when triggering the binding of the N-terminal region of Bcl-xL to the membrane interface. Thus, by truncating the TM helix, we aim to prevent the N-terminal domain of Bcl-xL from being anchored to the bilayer and, hence, ensure a detectable change in the fluorescent signal upon interaction of the donor and acceptor. Hereafter, the truncated construct of the protein will be simply termed Bcl-xL.

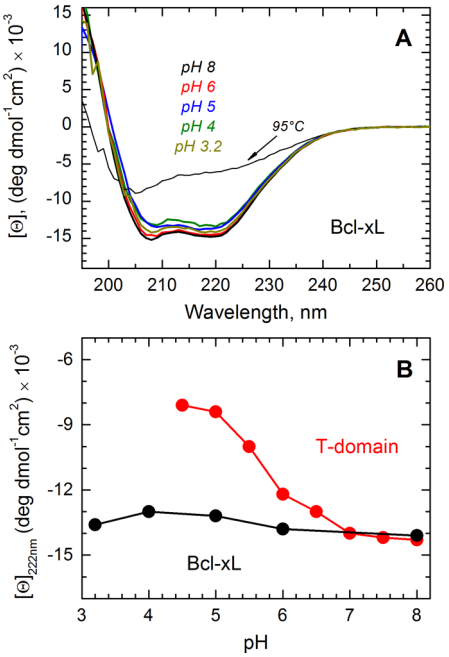

Figure 3. Comparison of the pH-dependent variation in the secondary structure and thermostability of Bcl-xL and the T-domain in solution. (A) CD spectra of Bcl-xL in solution at pH 8 (black), pH 6 (red), pH 5 (blue), pH 4 (olive), and pH 3.2 (dark yellow) at 25 °C. The CD spectrum at pH 8 and 95 °C is shown for reference. (B) pH-dependent changes in molar ellipticity measured at 222 nm for the T-domain (red symbols, data reproduced from ref 45 for visual comparison) and Bcl-xL (black symbols).

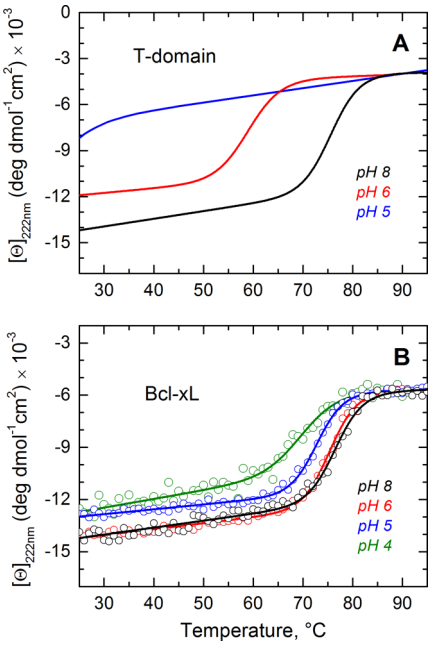

Figure 4. Comparison of the pH-dependent variation in the thermostability of Bcl-xL and the T-domain in solution (corresponding thermodynamic parameters are summarized in Table 1). (A) Fitting curves of the previously published data[17] upon thermal unfolding of the T-domain in solution at pH 8 and 6 are shown for reference. At pH 5, no cooperative melting transition can be detected. (B) Thermal unfolding of Bcl-xL at pH 8 (black), pH 6 (red), pH 5 (blue), and pH 4 (olive). The figure illustrates the small effect of acidification on the secondary structure of Bcl-xL, contrasting with the dramatic loss of stability of the T-domain.

pH-Dependent Stability in Solution. The diphtheria toxin T-domain inserts into the bilayer through pH-triggered conformational changes that occur in solution and in the membrane, going along multiple intermediate states until reaching the final transmembrane conformation.[13] The first conformational change occurs in solution with a midpoint pH of 6.2 and corresponds to the conversion of the water-soluble state (W-state) into the membrane-competent state (W^+-state) as a result of the protonation of key histidine residues.[2,14,16] The resulting W^+-state, while different from a molten globule state populated at pH <5 (as discussed in ref 2), is nevertheless characterized by partial refolding, a decrease in the amount of secondary structure, and a loss of thermostability.[14,16,17] To determine whether the pH-triggered membrane insertion of Bcl-xL goes through the formation of the same intermediate, we tested the pH-induced loss of secondary structure by CD spectroscopy (Figure 3A). The CD spectrum in solution at pH 8 has the typical features of an α-helical protein (black spectrum), consistent with the high-resolution structure in solution,[24] with minima of ellipticity at ~208 and ~222 nm and a maximum at ~190 nm. Upon acidification, the CD spectrum of Bcl-xL maintained its characteristic shape and exhibits a marginal decrease in molar ellipticity changes (Figure 3), indicating that Bcl-xL does not experience a pH-induced loss of secondary structure. This behavior is different from that of the T-domain (Figure 3B), which loses a substantial part of its ellipticity signal in the same pH range.[44,45]

We then tested the pH-induced loss of thermodynamic stability by measuring changes in ellipticity at 222 nm as a function of temperature. As the first step, we established that thermal unfolding of Bcl-xL is reversible and rate-independent (Figure S1 of the Supporting Information), which are prerequisites for quantitative analysis. To provide a visual reference, we display the fits for the previously published thermal unfolding data for the T-domain[17] in Figure 4A. These results indicate a substantial loss of stability when the pH is reduced from 8 to 6, which follows from a >15 °C decrease in the melting temperature and a decrease in transition enthalpy $\Delta H°$ (thermodynamic parameters for the thermal denaturation of both proteins are summarized in Table 1). The cooperative melting transition is no longer observed at pH 5, when the T-domain is converted to the W^+-state (Figure 4A, blue line). In contrast, we observe identical thermal transitions of Bcl-xL at pH 8 and 6 (Figure 4B). Moreover, further acidification up to pH 4 causes only a small decrease in the melting temperature and transition enthalpy (Figure 4B and Table 1). These results clearly indicate that the solution fold Bcl-xL is not destabilized by acid, complementing a previous report that showed Bcl-xL being equally resistant to chemical denaturation at neutral and acidic pH.[47] Together, our measurements suggest that Bcl-xL

Table 1. Thermodynamic Parameters for the Thermal Unfolding of the T-Domain and Bcl-xL in Solution at the Indicated pH

	T-domain[a]		Bcl-xL	
pH	T_m (°C)	$\Delta H°$ (kcal/mol)	T_m (°C)	$\Delta H°$ (kcal/mol)
8	75 ± 1	95 ± 7	77 ± 1	87 ± 6
6	59 ± 1	78 ± 6	76 ± 1	88 ± 4
5	no cooperative transition		73 ± 1	89 ± 4
4	no cooperative transition		70 ± 1	62 ± 8

[a]The parameters for the T-domain were previously published in ref 17.

dx.doi.org/10.1021/bi400926k | Biochemistry 2013, 52, 7901−7909

does not go through a CD-detectable pH-induced conformational change in the aqueous phase as does the T-domain, demonstrating the difference at the very early stages of the membrane insertion pathways.

Membrane Association. Previously, we have reported the pH dependence of membrane binding of the T-domain to vesicles of various lipid compositions using several independent spectroscopic methods, which produced results with excellent agreement.[13,16] One of them, based on a FRET methodology, is used here for Bcl-xL. Briefly, the donor dye (Alexa488) is attached to the protein, and the acceptor (Rhodamine) is incorporated into the lipid vesicle as Rhodamine-PE. When the protein and vesicles are mixed together at various pH values, the binding can be measured by the decrease in the emission intensity of the donor or by the shortening of its fluorescence lifetime. We show representative results of the steady-state (Figure 5A) and lifetime (Figure 5B) fluorescence measurements for membrane interaction of the Bcl-xL R102C mutant with the dye selectively attached to the cysteine residue. As expected, the data indicate a decrease in the fluorescence intensity and faster fluorescence decay when the interaction between the donor and acceptor is triggered by acidification [steps 1 (black) and 2 (blue)]. These spectral changes do not occur in the absence of the acceptor (Figure S2 of the Supporting Information) and therefore are consistent with the association of labeled Bcl-xL with the membrane. Importantly, the process is reversible, because the spectral features are recovered upon the return to pH 8 [step 3 (red)], allowing the thermodynamic treatment of the data.

For the T-domain, the initial binding proceeds through an interfacial intermediate I-state and is largely independent of the physicochemical properties of the membrane interface.[13] We tested whether this would also hold true for Bcl-xL by measuring the association of the protein to LUV with different lipid compositions as a function of pH. To do so, we used the FRET assay described above, and we calculated the FRET efficiency of binding at different pH values. [We have also tested whether the position of labeling affected this measurement by using three different single-cysteine mutants, G70C, R102C, and S110C. The resulting pH-dependent binding profiles are superimposable (Figure S3 of the Supporting Information), indicating that we can label any of the three residues with the donor dye without affecting membrane binding.] In Figure 6A, we show the titration curves previously obtained in the case of the T-domain,[13] where it is evidenced that regardless of the proportion of the anionic lipid POPG in the LUV, the p*K* of the transition remains mostly unaltered. The case of Bcl-xL (Figure 6B), however, appears to be different. In this case, the decrease in the POPG content causes a shift in the p*K* of the transition, indicating that the binding of the protein to the bilayer depends on the physicochemical properties of the membrane interface. Furthermore, Bcl-xL was unable to bind to LUV composed of only 10% anionic lipid (cyan), indicating that POPG is critical for binding of the protein to the membrane. Thus, in contrast to the case of the T-domain, our results indicate that the formation of the

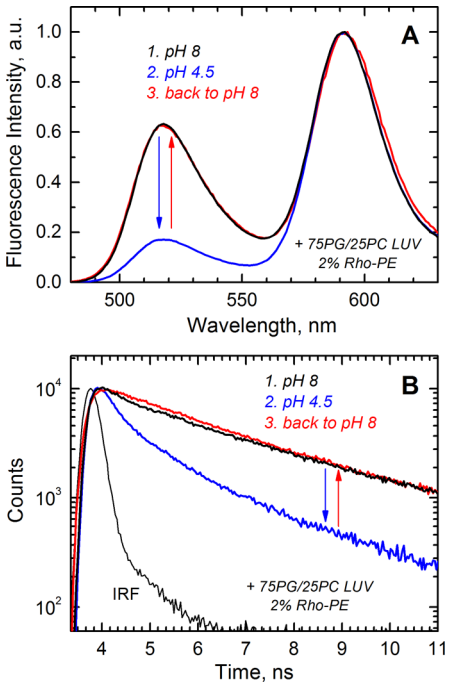

Figure 5. Reversibility of pH-dependent membrane association of Bcl-xL examined by the FRET measurements between donor-labeled protein and acceptor-labeled LUV. (A) Emission spectra of the donor at pH 8 (step 1, black) and pH 4.5 (step 2, blue) in the presence of the acceptor. The loss of intensity is recovered upon addition of NaOH to return to pH 8 (step 3, red). (B) Fluorescence decay of the donor at pH 8 (step 1, black) and pH 4.5 (step 2, blue) in the presence of the acceptor. The shortening of the decay is reversed upon the return to pH 8 (step 3, red). The data indicate that the pH-triggered binding of Bcl-xL to the membrane is a reversible process.

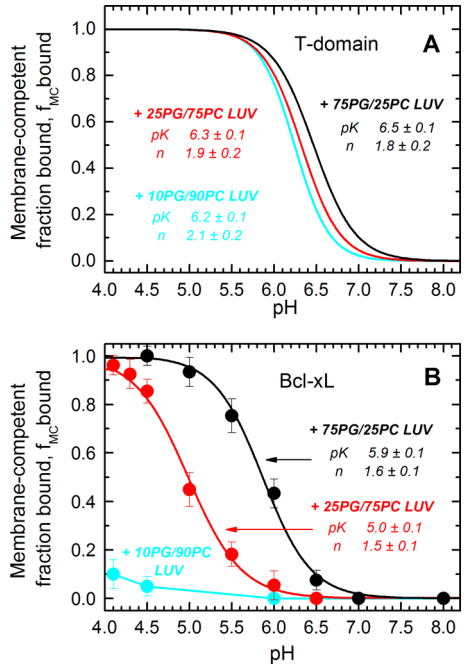

Figure 6. Comparison of pH-dependent binding of Bcl-xL and the T-domain to LUV composed of different mixtures of POPC and POPG. (A) The binding of the T-domain to the membrane interface does not depend on the mole fraction of POPG, as the three lipid compositions result in almost identical titration curves (only fitting curves taken from ref 13 are shown). (B) The titration curves of Bcl-xL shift to a lower pH when the mole fraction of POPG decreases from 75% (black) to 25% (red), with no detectable binding at 10% POPG (cyan). The p*K* and *n* (Hill coefficient) were obtained by fitting the data to a two-state model as described in Materials and Methods.

dx.doi.org/10.1021/bi400926k | *Biochemistry* 2013, 52, 7901−7909

membrane-competent state of Bcl-xL responds to changes in the physicochemical environment of the membrane interface.

This difference in the binding to the membrane interface implies that both proteins respond to the pH changes at different stages of the process. In the case of the T-domain, the protein would respond to acidification when still in the bulk solution because (1) the low pH causes conformational changes in the absence of membranes (Figures 3 and 4 and refs 14, 16, 17, and 44) and (2) binding to the bilayer does not depend on the physicochemical properties of the membrane interface (Figure 6 and ref 13). In the case of Bcl-xL, however, the opposite is true. (1) No changes are observed during the acidification in the absence of membranes (Figures 3 and 4), and (2) there is a strong dependence on the content of POPG (Figure 6). The charges on the POPG headgroup will create a negative surface potential that can either affect the pK_a values of key titratable groups of Bcl-xL directly, possibly modulate the local pH near the interface, or both.[48,49]

Membrane Insertion of the Hydrophobic Helical Hairpin. The next step in the insertion pathway of the T-domain is an interfacial refolding and membrane insertion of the hydrophobic helical hairpin TH8 of TH9 (Figure 1A, red helices) to form a transmembrane T-state.[13] The formation of this state can be followed experimentally by attaching the environment-sensitive fluorescent probe NBD to a single-cysteine mutant in the middle of helix TH9.[13,15] A similar transition is predicted to occur for Bcl-xL, as helices α5 and α6 (Figure 1B, red helices) have been observed to adopt a transmembrane topology in the context of the isolated fragments.[25] To confirm that these helices can be inserted in the context of protein, we labeled helix α6 at position N175C (Figure 1B) with NBD. We show a typical measurement in Figure 7, where the acidification of the medium in the presence of LUV [steps 1 (black) and 2 (blue)] results in a 12 nm blue shift and a 7-fold increase in the intensity in the emission spectra (Figure 7A), and a longer fluorescence decay (Figure 7B) of the NBD-labeled Bcl-xL. These spectral changes are consistent with the repositioning of the probe to a nonpolar environment, where the fact that it does not occur in the absence of LUV (Figure S4 of the Supporting Information) suggests that the spectral changes are the result of the probe being located within the hydrocarbon core. The return to pH 8.0 causes the recovery of the spectral features and lifetime decay, which indicates that this insertion process is reversible (step 3, red).

The pH dependence of this insertion is affected by the mole fraction of POPG in the T-domain, where a high proportion of anionic lipid is required for the protein to adopt the T-state.[13] In Figure 8A, we show the fitting curves for the pH dependence of the insertion of the T-domain as a reference. We made the parallel analysis for the hairpin of Bcl-xL by using the NBD-labeled protein as described above and measuring the changes in intensity as a function of the pH. The normalized data are presented in Figure 8B, where it is observed that the pH dependence varied just slightly with a decrease in the mole

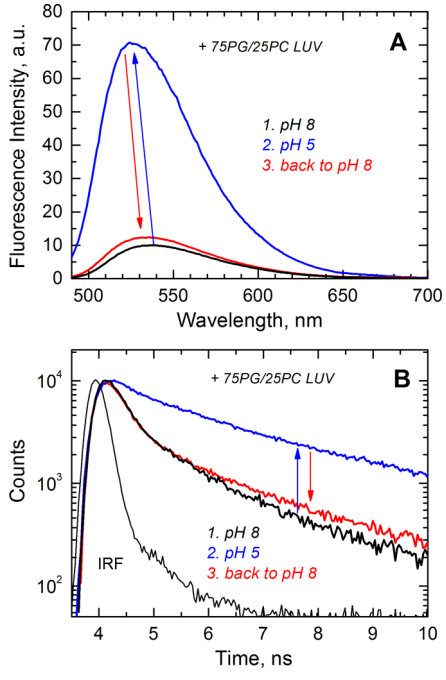

Figure 7. Reversibility of pH-dependent membrane insertion of Bcl-xL examined by a fluorescence assay based on the spectroscopic responses of the environment-sensitive probe NBD attached to residue N175C in the middle of helix α6. (A) Emission spectra in the presence of LUV at pH 8 (step 1, black) and 5 (step 2, blue). There is an increase in intensity and a blue shift at acidic pH in the presence of LUV, and a recovery of spectral features upon the return to pH 8 (step 3, red). (B) Fluorescence decay of the same samples illustrating the broadening of the decay at acidic pH in the presence of LUV.

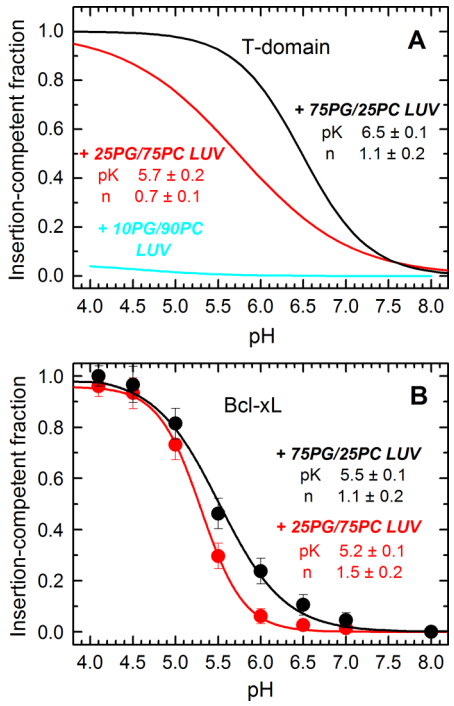

Figure 8. Comparison of pH-dependent membrane insertion of the hydrophobic helical hairpins of the T-domain and Bcl-xL. (A) The membrane insertion of the T-domain into LUV, determined as a function of pH, strongly depends on the mole fraction of POPG in the LUV (only fitting curves from ref 13 are shown). (B) The membrane insertion of Bcl-xL, studied as a function of the pH by following the changes in emission intensity at 525 nm, does not strongly depend on the POPG content of LUV (data in 90:10 POPC/POPG mixtures were omitted because there was no initial binding of the protein to LUV with this lipid composition). The data were fit to a two-state model as described in Materials and Methods.

dx.doi.org/10.1021/bi400926k | *Biochemistry* 2013, 52, 7901−7909

fraction of POPG in the membrane. The data for LUV composed of 10% POPG were excluded from the analysis because there were no spectral changes observed, because of the lack of association of Bcl-xL with the membrane under those conditions in the first place (see Figure 6B). The T-domain is fully bound to the membrane under those same conditions (see Figure 6A), and therefore, the lack of membrane insertion is due to the protein being trapped in a previous kinetic intermediate in the membrane interface. In contrast, pH dependencies of insertion of Bcl-xL only marginally differ from those of initial association, suggesting that the noninserted state on the membrane interface exists only transiently. Thus, the insertion of the helical hairpins also takes place by a different mechanism, where the T-domain responds to the presence of the anionic lipid for this step, but not Bcl-xL.

SUMMARY

We summarize our findings in Figure 9, where we illustrate the comparison of the insertion pathways for the T-domain and Bcl-xL. The structures of the soluble W-states are similar for the two proteins,[7,24] featuring a pair of long hydrophobic helices in the middle of the structure (colored red in Figure 1): TH8 and TH9 for the T-domain and α5 and α6 for Bcl-xL. While these helices will adopt a transmembrane conformation in the final inserted T-state in both cases, the similarities between the two proteins end there. For the case of the T-domain (Figure 9A), the folded soluble W-state is initially converted to the partially unfolded membrane-competent W^+-state as a result of acidification of the solution. This W^+-state then interacts with the membrane in a manner that is independent of the properties of the membrane interface, indicating that the initial pH-dependent conformational switching event occurs in solution.[13,16] The physiological benefit of this feature is likely to be related to the fact that the toxin may dissociate from its receptor inside the endosome[50] and the T-domain is no longer localized close to the membrane interface. The pathway proceeds through a series of intermediate states, such as the interfacial I-state and the activated insertion-competent I^+-state.[13] The final insertion into T-state is regulated by additional protonation on the membrane interface and by the presence of anionic lipids, presumably promoting formation of productive intermediates via electrostatic interactions with cationic groups on the T-domain.

Remarkably, the soluble W-state of Bcl-xL is not destabilized by acidification, and the formation of the membrane-competent state does not appear to require a conformational change to occur in solution (Figures 3 and 4). Unlike in the case of the T-domain, the conformational switching initiating the insertion cascade requires the membrane interface and is modulated by the presence of anionic lipids (Figure 6). (It is possible that this difference is related to the possibility that the protonation of acidic residues plays a more prominent role in case of Bcl-xL than in the case of the T-domain, for which histidine protonation has been established as a key factor modulating pH-dependent refolding and membrane insertion.[2,14−17] The exact molecular mechanism of lipid modulation of binding of Bcl-xL to membranes and the identity of the residues involved in pH-dependent conformational switching on the lipid−water interface, however, will be a subject of future studies involving mutagenesis and various lipid compositions.) Once the protein is on the interface, the insertion proceeds without the requirement of additional protonation in a lipid-independent

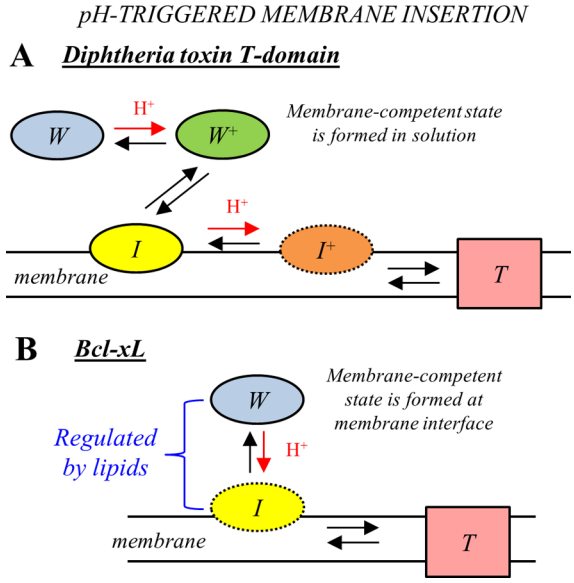

Figure 9. Schematic representations of the pH-triggered membrane insertion pathways of the diphtheria toxin T-domain (A) and apoptotic regulator Bcl-xL (B). Each starts with a similarly folded soluble W-state (Figure 1) and ends with membrane-inserted T-state, in which two central hydrophobic helices, TH8 and TH9 of the T-domain and α5 and α6 of the Bcl-xL, adopt a transmembrane conformation. The pathway connecting the two states, however, is very different in the two proteins. The T-domain goes through a set of intermediate states and undergoes several protonation transitions, both in solution and on the membrane interface, characterized by staggered pH dependencies.[13] Unlike the T-domain, Bcl-xL is not destabilized by acidic pH in solution, and protonation resulting in the formation of its membrane-competent form occurs on the membrane interface where it can be regulated by lipid composition. The interfacial intermediate state for Bcl-xL appears to be transient (as indicated by the dotted borderline of the I-state in the scheme) with insertion closely following initial association with the membrane interface (see Figures 6 and 8 and the text for details).

manner, which is again different from the behavior of the T-domain (Figure 8). Thus, our study clearly indicates that Bcl-xL and the diphtheria toxin T-domain insert into the lipid bilayer following different membrane insertion and protonation pathways. We suggest that the difference in the nature of the conformational switching in both proteins evolved to best serve their physiological function. For the T-domain, the robustness of delivery of its cargo (the catalytic domain, ultimately responsible for toxicity) requires no regulation step and is achieved by a single copy of the protein. In contrast, Bcl-xL and other proteins of the Bcl-2 family act collectively, and their function is very tightly regulated.[6,19,20] Subsequently, lipid-dependent triggering of the insertion (Figure 6) can be a part of such regulatory machinery. Another important aspect of membrane interactions of Bcl-xL is the complete reversibility of binding (Figure 5) and insertion (Figure 7), also suggested previously,[28] which may be required for proper functioning of this protein.

ASSOCIATED CONTENT

Supporting Information

Four figures. This material is available free of charge via the Internet at http://pubs.acs.org.

dx.doi.org/10.1021/bi400926k | Biochemistry 2013, 52, 7901−7909

AUTHOR INFORMATION

Corresponding Author

*E-mail: aladokhin@kumc.edu. Phone: (913) 588-0489. Fax: (913) 588-7440.

Funding

This research was supported by National Institutes of Health Grant GM-069783. M.V.-U. was partially supported by Fulbright-CONICYT.

Notes

The authors declare no competing financial interest.

ACKNOWLEDGMENTS

We thank Dr. Kenneth Peterson for the kind donation of cDNA obtained from K562 human lymphoma cells that served as a template for the cloning of Bcl-xL. We are grateful to Mr. M. A. Myers for his editorial assistance.

REFERENCES

(1) Murphy, J. R. (2011) Mechanism of diphtheria toxin catalytic domain delivery to the eukaryotic cell cytosol and the cellular factors that directly participate in the process. *Toxins 3*, 294−308.

(2) Ladokhin, A. S. (2013) pH-triggered conformational switching along the membrane insertion pathway of the diphtheria toxin T-domain. *Toxins 5*, 1362−1380.

(3) Young, J. A., and Collier, R. J. (2007) Anthrax Toxin: Receptor Binding, Internalization, Pore Formation, and Translocation. *Annu. Rev. Biochem. 76*, 243−265.

(4) Cramer, W. A., Heymann, J. B., Schendel, S. L., Deriy, B. N., Cohen, F. S., Elkins, P. A., and Stauffacher, C. V. (1995) Structure-function of the channel-forming colicins. *Annu. Rev. Biophys. Biomol. Struct. 24*, 611−641.

(5) Gerke, V., and Moss, S. E. (2002) Annexins: From structure to function. *Physiol. Rev. 82*, 331−371.

(6) Youle, R. J., and Strasser, A. (2008) The BCL-2 protein family: Opposing activities that mediate cell death. *Nat. Rev. Mol. Cell Biol. 9*, 47−59.

(7) Bennett, M. J., and Eisenberg, D. (1994) Refined structure of monomeric diphtheria toxin at 2.3 Å resolution. *Protein Sci. 3*, 1464−1475.

(8) Oh, K. J., Zhan, H., Cui, C., Hideg, K., Collier, R. J., and Hubbell, W. L. (1996) Organization of diphtheria toxin T domain in bilayers: A site-directed spin labeling study. *Science 273*, 810−812.

(9) Oh, K. J., Zhan, H., Cui, C., Altenbach, C., Hubbell, W. L., and Collier, R. J. (1999) Conformation of the diphtheria toxin T domain in membranes: A site-directed spin-labeling study of the TH8 helix and TL5 loop. *Biochemistry 38*, 10336−10343.

(10) Rosconi, M. P., Zhao, G., and London, E. (2004) Analyzing topography of membrane-inserted diphtheria toxin T domain using BODIPY-streptavidin: At low pH, helices 8 and 9 form a transmembrane hairpin but helices 5−7 form stable nonclassical inserted segments on the cis side of the bilayer. *Biochemistry 43*, 9127−9139.

(11) Senzel, L., Gordon, M., Blaustein, R. O., Oh, K. J., Collier, R. J., and Finkelstein, A. (2000) Topography of diphtheria toxin's T domain in the open channel state. *J. Gen. Physiol. 115*, 421−434.

(12) Wang, Y., Malenbaum, S. E., Kachel, K., Zhan, H. J., Collier, R. J., and London, E. (1997) Identification of shallow and deep membrane-penetrating forms of diphtheria toxin T domain that are regulated by protein concentration and bilayer width. *J. Biol. Chem. 272*, 25091−25098.

(13) Kyrychenko, A., Posokhov, Y. O., Rodnin, M. V., and Ladokhin, A. S. (2009) Kinetic intermediate reveals staggered pH-dependent transitions along the membrane insertion pathway of the diphtheria toxin T-domain. *Biochemistry 48*, 7584−7594.

(14) Rodnin, M. V., Kyrychenko, A., Kienker, P., Sharma, O., Posokhov, Y. O., Collier, R. J., Finkelstein, A., and Ladokhin, A. S. (2010) Conformational switching of the diphtheria toxin T domain. *J. Mol. Biol. 402*, 1−7.

(15) Rodnin, M. V., Kyrychenko, A., Kienker, P., Sharma, O., Vargas-Uribe, M., Collier, R. J., Finkelstein, A., and Ladokhin, A. S. (2011) Replacement of C-terminal histidines uncouples membrane insertion and translocation in diphtheria toxin T-domain. *Biophys. J. 101*, L41−L43.

(16) Kurnikov, I. V., Kyrychenko, A., Flores-Canales, J. C., Rodnin, M. V., Simakov, N., Vargas-Uribe, M., Posokhov, Y. O., Kurnikova, M., and Ladokhin, A. S. (2013) pH-Triggered Conformational Switching of the Diphtheria Toxin T-Domain: The Roles of N-Terminal Histidines. *J. Mol. Biol. 425*, 2752−2764.

(17) Vargas-Uribe, M., Rodnin, M. V., Kienker, P., Finkelstein, A., and Ladokhin, A. S. (2013) Crucial Role of H322 in Folding of the Diphtheria Toxin T-Domain into the Open-Channel State. *Biochemistry 52*, 3457−3463.

(18) Wang, C., and Youle, R. J. (2009) The role of mitochondria in apoptosis. *Annu. Rev. Genet. 43*, 95−118.

(19) Shamas-Din, A., Kale, J., Leber, B., and Andrews, D. W. (2013) Mechanisms of action of bcl-2 family proteins. *Cold Spring Harbor Perspect. Biol.*, 5.

(20) Garcia-Saez, A. J. (2012) The secrets of the Bcl-2 family. *Cell Death Differ. 19*, 1733−1740.

(21) Soriano, M. E., and Scorrano, L. (2011) Traveling Bax and forth from mitochondria to control apoptosis. *Cell 145*, 15−17.

(22) Edlich, F., Banerjee, S., Suzuki, M., Cleland, M. M., Arnoult, D., Wang, C., Neutzner, A., Tjandra, N., and Youle, R. J. (2011) Bcl-x(L) retrotranslocates Bax from the mitochondria into the cytosol. *Cell 145*, 104−116.

(23) Hsu, Y. T., Wolter, K. G., and Youle, R. J. (1997) Cytosol-to-membrane redistribution of Bax and Bcl-X(L) during apoptosis. *Proc. Natl. Acad. Sci. U.S.A. 94*, 3668−3672.

(24) Muchmore, S. W., Sattler, M., Liang, H., Meadows, R. P., Harlan, J. E., Yoon, H. S., Nettesheim, D., Chang, B. S., Thompson, C. B., Wong, S. L., Ng, S. L., and Fesik, S. W. (1996) X-ray and NMR structure of human Bcl-xL, an inhibitor of programmed cell death. *Nature 381*, 335−341.

(25) García-Sáez, A. J., Mingarro, I., Pérez-Payá, E., and Salgado, J. (2004) Membrane-insertion fragments of Bcl-XL, Bax, and Bid. *Biochemistry 43*, 10930−10943.

(26) Antignani, A., and Youle, R. J. (2006) How do Bax and Bak lead to permeabilization of the outer mitochondrial membrane? *Curr. Opin. Cell Biol. 18*, 685−689.

(27) Minn, A. J., Velez, P., Schendel, S. L., Liang, H., Muchmore, S. W., Fesik, S. W., Fill, M., and Thompson, C. B. (1997) Bcl-x(L) forms an ion channel in synthetic lipid membranes. *Nature 385*, 353−357.

(28) Thuduppathy, G. R., Terrones, O., Craig, J. W., Basanez, G., and Hill, R. B. (2006) The N-terminal domain of Bcl-xL reversibly binds membranes in a pH-dependent manner. *Biochemistry 45*, 14533−14542.

(29) Thuduppathy, G. R., Craig, J. W., Kholodenko, V., Schon, A., and Hill, R. B. (2006) Evidence that membrane insertion of the cytosolic domain of Bcl-xL is governed by an electrostatic mechanism. *J. Mol. Biol. 359*, 1045−1058.

(30) Garcia-Saez, A. J., Ries, J., Orzaez, M., Perez-Paya, E., and Schwille, P. (2009) Membrane promotes tBID interaction with BCL(XL). *Nat. Struct. Mol. Biol. 16*, 1178−1185.

(31) Billen, L. P., Kokoski, C. L., Lovell, J. F., Leber, B., and Andrews, D. W. (2008) Bcl-XL inhibits membrane permeabilization by competing with Bax. *PLoS Biol. 6*, e147.

(32) Gordon, M., and Finkelstein, A. (2001) The number of subunits comprising the channel formed by the T domain of diphtheria toxin. *J. Gen. Physiol. 118*, 471−480.

(33) Palchevskyy, S. S., Posokhov, Y. O., Olivier, B., Popot, J. L., Pucci, B., and Ladokhin, A. S. (2006) Chaperoning of Insertion of Membrane Proteins into Lipid Bilayers by Hemifluorinated Surfactants: Application to Diphtheria Toxin. *Biochemistry 45*, 2629−2635.

(34) Franzin, C. M., Choi, J., Zhai, D., Reed, J. C., and Marassi, F. M. (2004) Structural studies of apoptosis and ion transport regulatory proteins in membranes. *Magn. Reson. Chem. 42*, 172−179.
(35) Zhan, H., Oh, K. J., Shin, Y.-K., Hubbell, W. L., and Collier, R. J. (1995) Interaction of the isolated transmembrane domain of diphtheria toxin with membranes. *Biochemistry 34*, 4856−4863.
(36) Haugland, R. P. (1996) *Handbook of Fluorescent Probes and Research Chemicals*, 6th ed., Molecular Probes, Inc., Eugene, OR.
(37) Hope, M. J., Bally, M. B., Mayer, L. D., Janoff, A. S., and Cullis, P. R. (1986) Generation of multilamellar and unilamellar phospholipid vesicles. *Chem. Phys. Lipids 40*, 89−107.
(38) Mayer, L. D., Hope, M. J., and Cullis, P. R. (1986) Vesicles of variable sizes produced by a rapid extrusion procedure. *Biochim. Biophys. Acta 858*, 161−168.
(39) Posokhov, Y. O., and Ladokhin, A. S. (2006) Lifetime fluorescence method for determining membrane topology of proteins. *Anal. Biochem. 348*, 87−93.
(40) Ladokhin, A. S. (2009) Fluorescence spectroscopy in thermodynamic and kinetic analysis of pH-dependent membrane protein insertion. *Methods Enzymol. 466*, 19−42.
(41) Oh, K. J., Senzel, L., Collier, R. J., and Finkelstein, A. (1999) Translocation of the catalytic domain of diphtheria toxin across planar phospholipid bilayers by its own T domain. *Proc. Natl. Acad. Sci. U.S.A. 96*, 8467−8470.
(42) Ren, J., Kachel, K., Kim, H., Malenbaum, S. E., Collier, R. J., and London, E. (1999) Interaction of diphtheria toxin T domain with molten globule-like proteins and its implications for translocation. *Science 284*, 955−957.
(43) Ladokhin, A. S., Legmann, R., Collier, R. J., and White, S. H. (2004) Reversible refolding of the diphtheria toxin T-domain on lipid membranes. *Biochemistry 43*, 7451−7458.
(44) Rodnin, M. V., Posokhov, Y. O., Contino-Pepin, C., Brettmann, J., Kyrychenko, A., Palchevskyy, S. S., Pucci, B., and Ladokhin, A. S. (2008) Interactions of fluorinated surfactants with diphtheria toxin T-domain: Testing new media for studies of membrane proteins. *Biophys. J. 94*, 4348−4357.
(45) Kyrychenko, A., Rodnin, M. V., Vargas-Uribe, M., Sharma, S. K., Durand, G., Pucci, B., Popot, J. L., and Ladokhin, A. S. (2012) Folding of diphtheria toxin T-domain in the presence of amphipols and fluorinated surfactants: Toward thermodynamic measurements of membrane protein folding. *Biochim. Biophys. Acta 1818*, 1006−1012.
(46) Chenal, A., Savarin, P., Nizard, P., Guillain, F., Gillet, D., and Forge, V. (2002) Membrane protein insertion regulated by bringing electrostatic and hydrophobic interactions into play. A case study with the translocation domain of the diphtheria toxin. *J. Biol. Chem. 277*, 43425−43432.
(47) Thuduppathy, G. R., and Hill, R. B. (2006) Acid destabilization of the solution conformation of Bcl-xL does not drive its pH-dependent insertion into membranes. *Protein Sci. 15*, 248−257.
(48) Fernandez, M. S., and Fromherz, P. (1977) Lipoid pH indicators as probes of electrical potential and polarity in micelles. *J. Phys. Chem. 81*, 1755−1761.
(49) Posokhov, Y. O., Rodnin, M. V., Lu, L., and Ladokhin, A. S. (2008) Membrane insertion pathway of annexin B12: Thermodynamic and kinetic characterization by fluorescence correlation spectroscopy and fluorescence quenching. *Biochemistry 47*, 5078−5087.
(50) Brooke, J. S., Cha, J. H., and Eidels, L. (1998) Diphtheria toxin:receptor interaction: Association, dissociation, and effect of pH. *Biochem. Biophys. Res. Commun. 248*, 297−302.